Mon. Not. R. Astron. Soc. **000**, 000–000 (2003) Printed 2 February 2008 (MN LATEX style file v2.2)

The relativistic Fe emission line in XTE J1650–500 with *BeppoSAX*: evidence for black hole spin and light bending effects?

G. Miniutti[1⋆], A.C. Fabian[1], J.M. Miller[2,3]
[1] *Institute of Astronomy, University of Cambridge, Madingley Road, Cambridge CB3 0HA*
[2] *Harvard–Smithsonian Center for Astrophysics, 60 Garden Street, Cambridge MA 02138, USA*
[3] *NSF Astronomy and Astrophysics Postdoctoral fellow*

2 February 2008

ABSTRACT
We report spectral results from three *BeppoSAX* observations of the black hole candidate XTE J1650–500 during its 2001/2002 outburst. We find strong evidence for the presence of a broad and strongly relativistic Fe emission line. The line profile indicates an accretion disc extending down to two gravitational radii suggesting the presence of a rapidly rotating central Kerr black hole. Thanks to the broadband spectral coverage of *BeppoSAX*, we could analyse the 1.5–200 keV spectra of the three observations and report the presence of a strong reflection component from the accretion disc, which is totally consistent with the observed broad Fe emission line. The shape of the reflection component appears to be affected by the same special and general relativistic effects that produce the broad Fe line. We study the variation of the different spectral components from the first to the third observation and we find that they are well reproduced by a recently proposed light bending model.

Key words: black hole physics — X-rays: individual (XTE J1650–500) — X-rays: stars

1 INTRODUCTION

Black Hole Candidates (BHC) often exhibit transitions between different X–ray states, defined by their different spectral and temporal behaviour (Tanaka & Lewin 1995; van der Klis 1995; Méndez & van der Klis 1997; McClintock & Remillard 2003). Transitions between different X–ray states are believed to be mainly due to variations in the mass accretion rate. However, recent observations (see e.g. Homan et al. 2001) strongly suggest that a single parameter is not sufficient to explain the nature of the different states, and at least a second one must be considered, whose nature is still unclear. Black hole X–ray binaries appear to evolve through a continuous range of states whose general properties strongly depend mainly on the relative contribution and interplay between two main spectral components, i.e. a soft thermal disc component and a hard non–thermal power law component. In some cases the presence of a reflection component and/or of emission lines and edges has been observed suggesting reprocessing of the hard X–rays by cold material (generally identified with the accretion disc).

Here we report spectral results from three *BeppoSAX* observations of the BHC XTE J1650–500 during its 2001/2002 outburst. The X–ray transient XTE J1650–500 was first detected in outburst with the *Rossi X-Ray Timing Explorer* (*RXTE*) on 2001 September 5 (Remillard 2001). Optical and radio counterparts were identified by Castro–Tirado et al. (2001) and Groot et al. (2001), respectively. Subsequent observations revealed X–ray variability, a hard spectrum and quasi–periodic oscillations (QPOs) at a few Hz making the source a BHC , although the mass of the central object is still not well constrained by the data (Markwardt, Swank & Smith 2001; Revnivtsev & Sunyaev 2001; Wijnands, Miller & Lewin 2001). High frequency variability at about 250 Hz (and also likely at 250$\times$ 2/3 Hz) has also been detected (Homan et al. 2003). If the 250 Hz oscillation is interpreted as the orbital frequency at the innermost stable circular orbit, one can obtain a mass estimate of 8.2 $M_{\odot}$ for a non–rotating black hole. If a rotating black hole is considered, the black hole mass could well be much higher.

XMM–Newton observations close to the peak of the outburst in the very high state revealed the presence of a broad and asymmetric Fe emission line suggesting that the black hole in XTE J1650–500 is rapidly rotating (Miller et al. 2002a). Fe line diagnostics is potentially very important for constraining the accretion flow geometry, black hole spin and the nature and location of the primary source illuminating the accretion disc. Such diagnostics has already been used in both BHC (see for example Martocchia et al. 2002; Miller et al. 2003, 2002a,b,c) and active galaxies (see e.g. Tanaka et al. 1995; Wilms et al. 2001; Fabian et al. 2002 for the most remarkable case of MCG–6-30-15).

The *BeppoSAX* observations of the 2001/2002 XTE J1650–500 outburst were performed just before and after the *XMM–Newton* observation that revealed the presence of a relativistic Fe emission line. Our main purpose is to explore the Fe line energy band to confirm (or not) the *XMM–Newton* detection and to ob-

⋆ E-mail: miniutti@ast.cam.ac.uk

tain improved constraints from the broadband spectra; thanks to the broadband coverage of the *BeppoSAX* instruments, we present a self–consistent analysis of the 1.5–200 keV spectrum XTE J1650–500 during its 2001/2002 outburst.

2 OBSERVATIONS

XTE J1650–500 was observed 3 times by the Italian–Dutch satellite *BeppoSAX* (Boella, Butler & Perola 1997a) during 2001. Here we report on the three observations made on September 11 (obs. 1), September 21 (obs. 2) and October 3 (obs. 3). For comparison, we note that the *XMM–Newton* observation by Miller et al. 2002 that revealed the presence of a broad, relativistic Fe line was performed on September 13. In this paper, data from the imaging instruments (LECS Parmar et al. 1997 and MECS Boella et al. 1997b) and from the collimated PDS (Frontera et al. 1997) instrument are reported. The data files have been obtained from the *BeppoSAX* public archive. Spectra for the LECS and MECS instruments are obtained within a circular region centred on the source with radius of 8 arcmin. The background was extracted from event files of source–free regions of the same size. Spectra were grouped such that each bin contains at least 20 counts. Exposures times for LECS were of 20 ks, 14 ks and 7 ks (obs. 1,2 and 3 respectively), while the MECS exposures were of 47 ks, 64 ks and 28 ks. The PDS exposure times were of 21 ks, 31 ks and 12 ks. The *BeppoSAX* data were fitted by using the XSPEC 11.2 package (Arnaud 1996). In the following, all the quoted uncertainties on the parameters correspond to 90 per cent confidence intervals for one interesting parameter ($\Delta\chi^2 = 2.71$).

3 SPECTRAL ANALYSIS

We first analysed the MECS data in the 2.5–10 keV energy band in order to look for the presence of a broad Fe emission line as observed in the September 13 *XMM–Newton* observation by Miller et al. (2002a). Some feature is present in the MECS data below 2.5 keV, independently of the spectral model that is used to analyse the data. We thus decided to ignore the low energy data below 2.5 keV and focus on the iron line energy band. To better constrain the continuum and to assess the relevance of reflection components in the spectra, we then added the PDS data in the range 13–200 keV. Some data from the LECS instruments (1.5–3.0 keV) have also been considered and we report our analysis of the broadband 1.5–200 keV data (LECS + MECS + PDS).

3.1 The 2.5–10 keV spectrum from the MECS instrument

We first analysed the MECS data by considering the "standard" model for galactic black hole candidates X–ray sources, i.e. a multicolour accretion disc blackbody (MCD) from Mitsuda et al. (1984) and a power law, modified by absorption in the interstellar medium (the PHABS model in XSPEC). The fit is very poor for the first two observations ($\chi^2 = 958$ and $\chi^2 = 422$, respectively) and better for obs. 3 ($\chi^2 = 200$) for 156 degrees of freedom. The main reason for the low quality of the fits is the presence of large residuals in the region of the Fe complex, above 3.5–4 keV. The shape of the residuals strongly suggest the presence of a broad and asymmetric Fe emission line in the three observations.

We then describe the 2.5–10 keV MECS data by adding the LAOR model to account for relativistic iron line emission from an accretion disc around a Kerr black hole. In this model, the emissivity profile on the accretion disc is described by a power law of the form $\epsilon(r) = r^{-\beta}$, where the emissivity index β is a free parameter of the model. After some testing, the inclination was fixed to 45 degrees (as in Miller et al. 2002) as the data indicate clear preference for intermediate inclinations. The outer disc radius was fixed to its maximum possible value of $400\ r_g$, where $r_g = G\,M/c^2$ and M is the black hole mass. The inner disc radius, the emissivity index, the rest energy of the emission line, and the model normalisation were let free to vary during the fit. A smeared edge (SMEDGE) was also added to the model. This phenomenological model for the absorption edge is here considered for comparison with previous works only. A more physically–motivated reflection component will be considered in the next Section where the 1.5–200 keV spectra are discussed.

The addition of the SMEDGE and LAOR components significantly improved the fit ($\chi^2 = 158$, $\chi^2 = 197$, and $\chi^2 = 149$ for obs. 1, 2, and 3 respectively, for 149 degrees of freedom) with respect to our initial model (DISKBB + POWERLAW). However, some positive residuals are still found in the Fe line band, suggesting the presence of an emission feature around 5 keV. We then added a narrow Gaussian (with fixed zero width) and we detected emission features at 5.4 keV in obs. 1 and at 5.2 keV in obs. 2 and 3. The narrow line EW is small (less than 20 eV), but its inclusion in the model improves the statistic ($\Delta\chi^2 \simeq 9 - 12$ depending on the observation with two less degrees of freedom). Its possible origin is discussed below. The results of the spectral analysis are reported in Table 1 as MODEL 1. Taking into account the three observations, the effective neutral hydrogen column density is found to be $N_H = (\ 0.5 \pm 0.1) \times 10^{22}$ atoms cm^{-2}.

In Fig. 1, to demonstrate the presence of the broad Fe line in the data, we show the data/model ratio obtained ignoring the 4-8 keV band in fitting the model. The data have then be re–inserted to show the broad residuals indicating that a relativistic Fe emission line is present in the data, as detected with *XMM–Newton* by Miller et al. (2002).

3.1.1 The broad Fe line

The LAOR model best–fit parameters indicate the presence of a relatively strong and highly relativistic iron line with equivalent width of about $EW \simeq 300$ eV. The line energy in obs. 2 and 3 indicates a high level ionisation, while in obs. 1 it suggests emission from less ionised iron. The emissivity profile on the accretion disc is well described by a steep power law with index $\beta \simeq 4 - 5$. This steep emissivity is consistent with previous measurements with *XMM–Newton* (Miller et al. 2002a) and strongly suggests that the accretion disc is illuminated by a centrally concentrated source of primary hard X–rays that strongly irradiates the inner disc region.

The Fe emission line profile indicates emission from an accretion disc extending down to about $2\ r_g$. Such a small inner disc radius is not consistent with a non–rotating Schwarzschild black hole if the accretion disc is assumed to extend down to the marginal stable orbit ($6\ r_g$ for a Schwarzschild black hole). On the other hand, since the marginal stable orbit for a maximally rotating Kerr black hole has a radius of about $1.24\ r_g$, the data suggest the presence of a central rapidly rotating Kerr black hole. However, the measure of an inner disc radius smaller than $6\ r_g$ does not necessary mean that the black hole must be spinning. Indeed, Reynolds & Begelman (1997) showed that the line profile from an accretion disc around a Schwarzschild black hole can be very similar to the one computed

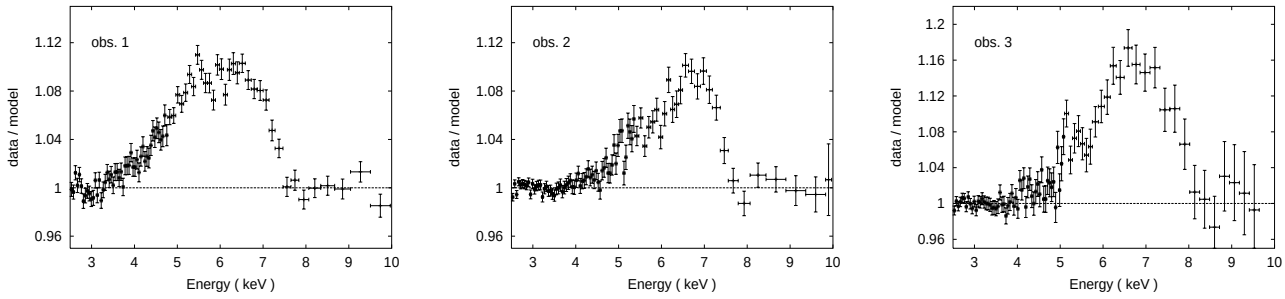

Figure 1. 2.5–10 keV data/model ratio obtained with a multicolour disc black body component, a power law and a smeared edge modified by photoelectric absorption for the three *BeppoSAX* observations. The 4–8 keV band, where emission line features are expected, has been ignored in fitting the model. Ratios have been rebinned for visual clarity.

in the Kerr spacetime, if emission within the marginal stable orbit is considered (but see Young, Ross & Fabian 1998).

3.1.2 The features around 5 keV

As discussed above, a narrow emission line at 5.4 ± 0.1 keV is formally required in obs. 1, while the line energy is 5.2 ± 0.2 keV in obs. 2 and 3. Although the measured EW is low, these features worth a brief comment. More than a single interpretation is of course possible both as emission around 5.2–5.4 keV or as absorption at slightly higher energies (for a similar feature in NGC 3516 see Nandra et al. 1999). Narrow emission lines with $E < 6.4$ keV are also seen in active galaxies (e.g. Turner et al. 2002, 2004; Guainazzi 2003; Yaqoob et al. 2003; Dovčiak et al. 2004). The 5.2–5.4 keV features in XTE J1650–500 could part of the main broad relativistic line. If, as it is likely, the emissivity on the disc is more complex than a simple power law, it is possible that some small features of the line profile are not well described by the LAOR model. Redshifted iron emission from an outflow, absorption due to resonant scattering in infalling material, or spallation of iron producing a fluorescent Cr emission line (Skibo 1997) provide other interesting possibilities.

On the other hand, since the Fe line profile is very broad, an explanation in terms of emission from the inner accreting flow seems likely. It ispossible that the observed features are due to redshifted Fe K_α emission line from the accretion disc, superimposed to the main broad Fe line component. As an example, a strong flare originating very close to the disc surface will illuminate only a very small region of the disc. The emissivity profile would thus comprise two components, a power law emissivity due to the illumination of the whole disc by the corona emission (producing the broad Fe line) and a small bump at the radius where the flare is active. If this is the case, we would mainly observe the blue horn of the emission line associated with the flare, the red wing being faint and confused with that of the main broad Fe line component. We tested this possibility by replacing the narrow Gaussian with a second LAOR line with energy and inclination tied to that of the main component and found results comparable to those reported in Table 1 if the 5.2-5.4 keV line comes from a narrow ring around 2–3 r_g. Since the quality of the data does not allow to distinguish between the different possibilities, we will not discuss them any further. We however include in our modelling a Gaussian emission line with fixed zero width at 5.2-5.4 keV, depending on the observation.

3.2 The broadband 1.5–200 keV spectrum of XTE J1650–500

In order to better constrain the Fe line parameters, a careful analysis of the underlaying continuum is necessary. It is clear that a power law and a SMEDGE model are simple, and probably too rough, approximations to the hard spectral shape. In particular, the presence of the Fe line strongly suggests that a reflection continuum due to reprocessing of the primary X–rays by the accretion disc, is present in the data. The 2.5–10 keV energy band is too limited to constrain the reflection continuum, and for this reason we consider the high energy data from the PDS instrument as well (in the range 13–200 keV). We also add some low energy data (1.5 to 3 keV) from the LECS instrument, to better constrain the thermal component of the spectrum. At lower energies, some absorption/emission features are visible. We decide to ignore these features in this analysis that is focused on the Fe complex and does not benefit much from the data below 1.5 keV.

The extension of the previous model (MODEL 1) to the 1.5–200 keV band does not provide a very good description to the data. The main reason is the presence of spectral curvature and positive residuals above 20 keV. The shape of the residuals suggests the presence of a Compton hump due to a reflection component. Because of the presence of these residuals and of the relativistic Fe emission line, and anticipating the presence of a ionised disc as suggested by the Fe line rest energies (see Table 1), we add a reflection component (PEXRIV, from Magdziarz & Zdziarski 1995) to our model, and remove the phenomenological SMEDGE model.

Moreover, as all the components emitted from the accretion disc should be affected by the same relativistic effects, the reflection component, the thermal disc black body component and a narrow (i.e. with fixed zero width) Gaussian emission line are relativistically "blurred" by convolving it with the core of the LAOR model. The width of the Gaussian emission line is fixed to zero because the Fe line profile is dictated by the effects of the relativistic blurring; our description of the Fe emission line is completely equivalent to the one provided by the LAOR model. The incident continuum is described by a power law with high energy cutoff; the photon index, cutoff energy and normalisation are tied to those of the PEXRIV model. We also include a (non–blurred) narrow emission line to model the features at $5.2 - 5.4$ keV, as discussed in the 2.5–10 keV analysis.

All abundances in the reflection model were fixed to solar values while the relative normalisation between incident power law and reflection (the relative reflection R) was let free to vary during the fit. The outer disc radius was fixed at 400 r_g and the inclina-

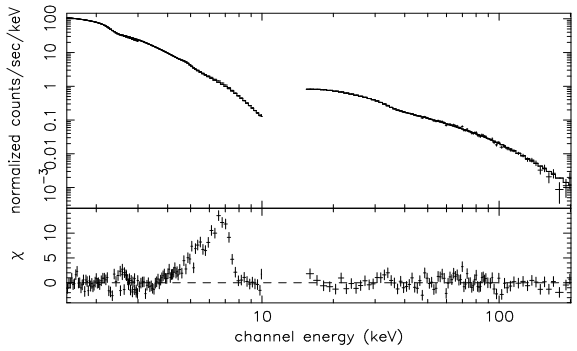

Figure 2. The 1.5–200 keV spectrum of obs. 2 and the data/model ratio (in terms of σ) obtained with our MODEL 2 when the 4–8 keV band is ignored in the fitting. The data have been rebinned for visual clarity.

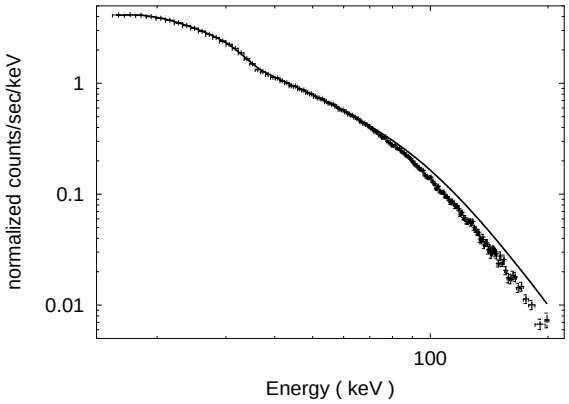

Figure 3. The 15–200 keV spectrum of obs. 1 from the PDS instrument demonstrates that our MODEL 2 is inappropriate to describe the data above 60–70 keV. A much sharper cutoff than the one provided by the CUTOFFPL model is needed.

tion at 45 degrees, as before. We notice also that the same model was used by Miller et al. 2002 to describe the September 13 *XMM–Newton* data. Hereafter we shall refer to this model as MODEL 2.

This model works well on the data of obs. 2 and 3 ($\chi^2/dof = 533.5/434$ and $\chi^2/dof = 434.8/416$, respectively) but a reasonable fit can be obtained for obs. 1 only up to about 60 keV ($\chi^2/dof = 402.5/324$). In obs. 1 a sharp feature is detected around 35 keV in the PDS data and is most likely instrumental. If the associated energy band is ignored in fitting the spectrum, the statistics is much better ($\chi^2/dof = 317.8/314$) and fit parameters are unaffected. However, the main problem for obs. 1 is that, if higher energy data above 60 keV are included, MODEL 2 fails to give an appropriate description of the spectrum. We shall report now our results with MODEL 2, restricting the energy band to 1.5–60 keV for obs. 1, and discuss later in some detail the broadband spectrum for this first observation. The results of the fits with MODEL 2 are reported in Table 2.

We measure an increase in the photon index from $\Gamma = 1.81$ in obs. 1 to $\Gamma \simeq 2.1$ in obs. 2 and 3 which is consistent with the general trend obtained by Rossi et al. (2003) from the analysis of *RXTE* observations during the same outburst, and an inner black body temperature of $0.6 - 0.7$ keV. The data support the presence of a reflection component that contributes significantly to the hard flux, especially during obs. 2 and 3 where the reflection fraction R is significantly greater than unity: the trend is of increasing R with time, from obs. 1 ($R \simeq 0.8$) to obs. 2 ($R \simeq 2.1$) and 3 ($R \simeq 2.9$). The large values of the relative reflection measured in obs. 2 and 3 indicate that the accretion disc is viewing more illuminating radiation than we actually detect in the power law component. The surface disc temperature and the ionisation parameter (ξ) of the reflection model vary in the range $1 - 9 \times 10^6$ K and $0.2 - 1.6 \times 10^4$ erg cm/s, respectively. Although these values are not well constrained by the data a trend of increasing ξ from obs. 1 to 3. is observed (see Table 2). Since the X–ray flux decreases from obs 1 to 3 (see Section 4 and Table 3) this indicates that the ionisation parameter is not correlated with flux. A possible explanation for the behaviour of R and ξ is given in Section 4.

Once again, the most relevant results concern the broad iron emission line. In all observations, the line emission is consistent with the disc extending down to about 2 gravitational radii suggesting the presence of a rapidly rotating Kerr black hole. Replacing the LAOR kernel with the DISKLINE one which describes a non–rotating Schwarzschild black hole, and fixing the inner disc radius at 6 r_g results in a worse description of the spectra (the smallest variation is $\Delta\chi^2 = 17$ with one more degree of freedom in obs. 3, while the largest occurs in obs. 1 with $\Delta\chi^2 = 70$). We stress again that $r_{\rm in}$ is measured not only through the iron line but is the result of the fit on all the components that are thought to originate from the accretion disc that are blurred with relativistic effects, so that the significance of the measured $r_{\rm in}$ is, in our opinion, enhanced. The PEXRIV model (lacking comptonisation) predicts too sharp an edge at high levels of ionisation and could thus require extreme relativistic blurring at high ionisation to smooth it out. However, the measured β and $r_{\rm in}$ do not show any trend toward extreme values as the ionisation parameter increases from obs. 1 to 3 by nearly one order of magnitude, so that we are confident about the robustness of our results. The emissivity index and the inner disc radius are both consistent with being constant from obs. 1 to 3.

The line EW is about 200 eV, depending on the observation and it is smaller than in the analysis of the 2.5–10 keV data (see Table. 1). This is mainly due to the non negligible contribution of the ionised reflection continuum in the Fe line region. The emissivity profile of the disc is quite steep ($\beta \simeq 3.5 - 3.8$) suggesting that the iron line emission is concentrated in the inner regions of the accretion disc. Summarising, our results confirm the evidence for the presence of a Kerr black hole rotating close to its maximum possible angular momentum ($a = 0.998$) in XTE J1650–500 as shown in the *XMM–Newton* observation by Miller et al. (2002), although other interpretations may still be viable (Reynolds & Begelman 1997). As an example, the broadband 1.5–200 keV spectrum of obs. 2 is shown in Fig. 2: the model is fitted ignoring the Fe line energy band between 4 and 8 keV. This energy range is then re–inserted to show the residuals in the Fe line region.

3.2.1 The 1.5–200 keV spectrum of observation 1

As already mentioned, MODEL 2 does not provide a good description of obs. 1 if data above 60 keV are included in the analysis. The reason of the failure is clearly shown in Fig. 3, where we show the PDS spectrum when the 1.5–60 keV best fit model for obs. 1 is extended up to 200 keV. The data in obs. 1 clearly require a sharper cutoff above 60 keV than the one provided by the exponentially decaying power law and reflection. Even if the high

energy cutoff of the CUTOFFPL and PEXRIV models is forced to assume low values, a reasonable fit can not be found. The sharp cutoff is most likely the sign of a comptonised continuum which is only roughly approximated by the exponentially cutoff power law. For simplicity, we describe the sharp break with a simple phenomenological model replacing the PEXRIV + CUTOFFPL model with a BEXRIV + BROKENPL, i.e. assuming a broken power law illuminating spectrum. The model provides a reasonable description to the broadband spectrum of the first *BeppoSAX* observation (with $\chi^2/dof = 516.0/448$) without changing the results of the 1.5–60 keV analysis reported in Table 2. The difference is the presence of a break energy at about 70 keV where the photon index changes. Above that energy, the photon index steepens from $\Gamma_{\rm low} \approx 1.8$ to $\Gamma_{\rm high} \approx 2.6$. As before, ignoring the PDS sharp feature energy band around 35 keV gives a much better fit with $\chi^2/dof = 428.5/438$. The spectral break is not visible in obs. 2 and 3 probably because of the lower signal to noise ratio in the PDS data that does not allow to constrain the shape above 60 keV well enough.

4 FE LINE VARIABILITY: EVIDENCE FOR LIGHT BENDING ?

In this Section, we investigate the correlations between the Power Law Component (PLC) that illuminates the accretion disc and the reprocessed Reflection Dominated Component (RDC), i.e. reflection continuum and the iron line.

In the three observations, we observe that the contribution of the black body component to the total flux gradually increases with time, while the PLC contribution shows the opposite trend. The 1.5–200 keV flux of the black body component increases by about one order of magnitude, while the PLC flux decreases by an even larger amount (see Table 3). As already mentioned, the relative reflection R increases by about a factor 3 as the PLC decreases from obs. 1 to 3, suggesting that R is anti–correlated with the PLC flux.

Our results are difficult to explain in the framework of the standard view of reflection models because any RDC emitted from the accretion disc is expected to respond to changes in the illuminating flux (the PLC), so that R should remain constant as the PLC flux changes. However, this picture is probably oversimplified and fails (for example) to account for the variability of the Seyfert 1 galaxy MCG–6-30-15. As already pointed out by Miller et al. (2002), this AGN exhibits some clear similarities with XTE J1650–500. In particular, it is characterised by an extremely broad iron emission line (strongly suggesting the presence of a Kerr black hole) and a steep emissivity profile (Wilms et al. 2001; Fabian et al. 2002). MCG–6-30-15 exhibits also a peculiar variability behaviour: in its normal states the spectral variability can be accounted for by a phenomenological model comprising a PLC that varies in normalisation and an almost constant RDC (and iron line) (Shih, Iwasawa & Fabian 2002; Fabian & Vaughan 2003; Taylor, Uttley & McHardy 2003). In low flux states, the iron line is correlated with the PLC (Reynolds et al. 2003). This behaviour has been successfully reproduced in terms of a light bending model in which general relativistic effects strongly affect the emission in the near vicinity of the central Kerr black hole (Miniutti et al. 2003; Miniutti & Fabian 2004).

The basic idea of the light bending model is that the PLC variability is mostly due to changes in the height of a centrally concentrated primary source of hard X–rays above the accretion disc rather than to changes in its intrinsic luminosity. If the source

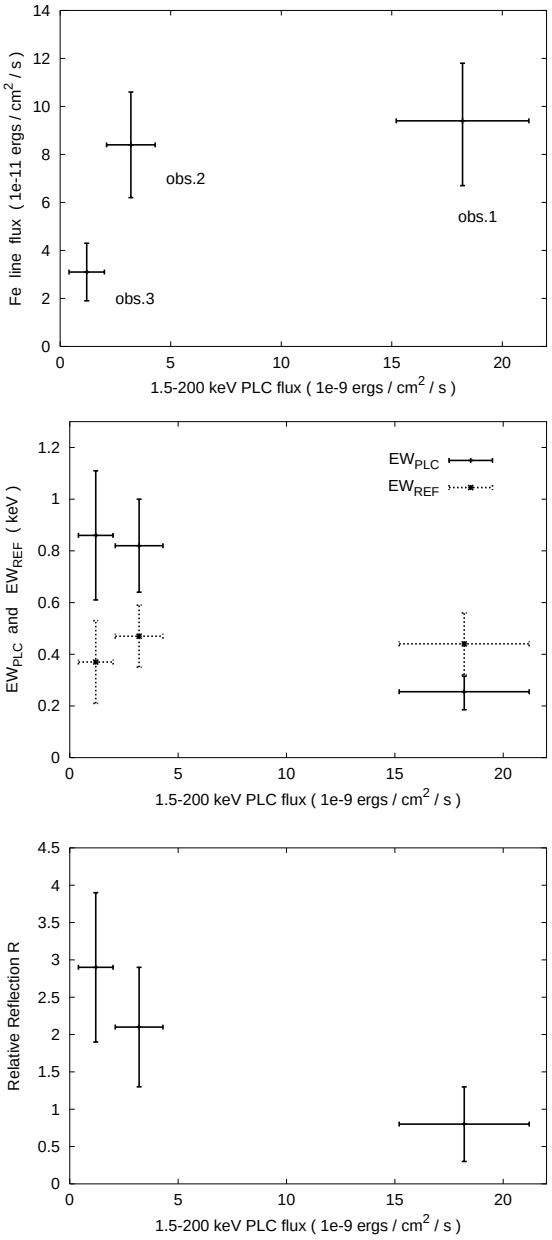

Figure 4. From top to bottom, we show, as a function of the 1.5–200 keV flux of the PLC: i) the Fe line flux; ii) the Fe line EW computed with respect to the PLC only ($\rm EW_{PLC}$) and with respect to the reflection continuum only ($\rm EW_{REF}$); iii) the relative reflection R. The obs. number is showed in the top panel and refers to the other two figures as well. Results are discussed in the text.

height is small (few gravitational radii), most of the radiation is bent onto the accretion disc by the strong gravitational field of the central black hole: this strongly reduces the observed PLC at infinity and enhances the illumination of the disc. The Fe line (and any RDC) varies with much smaller amplitude than the PLC and different regimes can be identified in which the line is correlated with the PLC, almost constant, or anti–correlated with the PLC. These regimes correspond to low, medium and high PLC flux states.

A major prediction of the model is that the hard spectrum becomes more and more reflection dominated as the PLC drops (i.e. as the height of the primary source decreases) so that the relative

reflection R increases as the system goes into low PLC flux states. Large values of the relative reflection are naturally expected in low PLC flux states. Thus, if the PLC variability can be accounted for by light bending, the increase of the relative reflection (and its large value) as the PLC flux drops from obs. 1 to 3 can be understood. Moreover, as the source height decreases and the PLC drops, the inner regions of disc are more and more illuminated, so that a reasonable expectation is that the ionisation parameter of the disc increases. This may explain the trend of increasing ionisation parameter from obs. 1 to 3 (see Table 2).

The model predicts that the Fe line flux is correlated with the PLC in low flux states, while it is almost constant in higher flux states. Furthermore, the Fe line EW should correlate with the reflection fraction, or in other words, the EW computed with respect to the reflection continuum only ($\mathrm{EW_{REF}}$) is predicted be roughly constant because, as in any reflection model, Fe line and RDC are expected to vary together. On the other hand, since the Fe line is predicted to vary much less than the PLC, the EW computed with respect to the PLC only ($\mathrm{EW_{PLC}}$) should be anti–correlated with the PLC and saturate only at low fluxes where Fe line and power law component are correlated.

As a test of the model, we then measure the Fe line flux, the PLC flux, $\mathrm{EW_{REF}}$, and $\mathrm{EW_{PLC}}$. Results are shown in Table 3 and Fig. 4: as predicted by the light bending model, the Fe line appears to be correlated with the PLC in low flux states and to saturate at higher flux levels (top panel of Fig. 4). Moreover, $\mathrm{EW_{REF}}$ is almost constant, while $\mathrm{EW_{PLC}}$ is anti–correlated with the PLC flux and possibly saturates at very low PLC flux, in excellent agreement with the model (middle panel). As already mentioned, the relative reflection R is anti–correlated with the PLC flux (bottom panel of Fig. 4).

Clearly, three observations are not enough to establish correlations properties with high level of significance. However, the behaviour of the iron line flux with respect to the PLC flux in XTE J1650–500 has been also measured with *RXTE* during the same 2001/2002 outburst and results are reported by Rossi et al. (2003) where 176 pointed observations are discussed. The observed Fe line vs. PLC behaviour is remarkably similar to our present results and to the predictions of the light bending model (see e.g. Figure 5 of Rossi et al. 2003 and Figure 2 of Miniutti & Fabian 2004). Of course, this does not mean that light bending is really at work in this source and that other models can not explain the correlation properties. However, the strong similarity between theoretical predictions and observational data is manifest.

5 DISCUSSION AND CONCLUSIONS

We present a broadband spectral analysis of the BHC XTE J1650–500 during its 2001/2001 outburst. The three *BeppoSAX* observations cover about 25 days starting from 2001 September 11, only a few days after the peak of the outburst. We have observed a broad Fe line profile in all three observations, confirming the detection with *XMM–Newton* by Miller et al. (2002a) during the very high state on 2001 September 13. The Fe line profile we observe strongly suggests that the accretion disc extends down to $r_{\rm in} \approx 2$, well within the limit of marginal stability for a non–rotating Schwarzschild black hole, thus indicating that XTE J1650–500 harbours a rapidly rotating (possibly maximally rotating) Kerr black hole.

The Fe line emission is consistently associated with a strong reflection spectral component from the accretion disc. The reflection dominated spectrum is also distorted by the special and general relativistic effects in the vicinity of the central black hole in the same way as the Fe line. The emissivity profile of the disc seems to be steeper than expected from standard disc models ($\beta \approx 3$) suggesting that the primary source that illuminates the disc is centrally concentrated.

From the first to the third observation, the power law component of the spectrum drops by more than one order of magnitude. In the same time, the relative reflection increases by a factor 3, suggesting that the spectrum becomes more and more reflection dominated as the power law flux decreases. We interpret this behaviour in terms of a light bending model for the variability of X–ray sources that has been presented elsewhere (see Miniutti et al 2003, 2004). The variability of the Fe line flux and EW is also consistent with the predictions of this model and with previous observations (Rossi et al. 2003).

ACKNOWLEDGEMENTS

GM thanks Kazushi Iwasawa for constructive discussions and Alessandra de Rosa for her help with *BeppoSAX* data analysis. We thank the referee, Chris Done, for helpful comments and the *BeppoSAX* Scientific Data Centre. GM thanks the PPARC for support. ACF thanks the Royal Society for support. JMM thanks the NSF for support through its AAPF program.

REFERENCES

Arnaud K.A., 1996, in ASP Conf. Ser. 101: Astronomical Data Analysis Software and Systems V, 5, 17
Boella G., Butler R.C., Perola G.C., 1997a, A&AS, 112, 299
Boella G. et al. 1997b, A&AS, 112, 327
Castro–Tirado A.J., Kilmartin P., Gilmore A., Petterson O., Bond I., Yock P., Sanchez–Fernandez C., 2001, IAU Circ., 7707, 3
Dovčiak M., Bianchi S., Guanazzi M., Karas V., Matt G., 2004, MNRAS in press, preprint (astro-ph/0401607)
Fabian A.C. et al., 2002, MNRAS, 335, L1
Fabian A.C., Vaughan S., 2003, MNRAS, 340, L28
Fiore F., Guainazzi G., Grandi P., 1999, Cookbook for *BeppoSAX* NFI Spectral Analysis. SDC report (http://asdc.asi.it/bepposax/software/index.html)
Frontera F., Costa E., dal Fiume F., Feroci M., Nicastro L., Orlandini M., Palazzi E., Zavattini G., 1997, A&AS, 112, 357
Groot P., Tingay S., Udalski A., Miller J., 2001, IAU Circ., 7708, 4
Guainazzi M., 2003, A&A, 401, 903
Homan J., Wijnands R., van der Klis M., Belloni T., van Paradijs J., Klein–Wolt M., Fender R., Méndez M., 2001, ApJS, 132, 377
Homan J., Klein–Wolt M., Rossi S., Miller J.M., Wijnands R., Belloni T., van der Klis M., Lewin W.H.G., 2003, ApJ, 586, 1262
Markwardt C., Swank J., Smith E., 2001, IAU Circ., 7707, 2
Martocchia A., Matt G., Karas V., 2002, A&A 383, L23
McClintock J.E., Remillard R.A., to appear in Compact Stellar X–ray sources eds. W.H.G. Lewin and M. van der Klis, preprint (astro-ph/0306213)
Méndez M., van der Klis M., 1997, ApJ, 479, 926
Miller J.M. et al., 2002a, ApJ, 570, L69
Miller J.M., Fabian A.C., in'tZand J.J.M., Reynolds C.S., Wijnands R., Nowak M.A., Lewin W.H.G., 2002b, ApJ, 577, L15
Miller J.M. et al., 2002c, ApJ, 578, 348
Miniutti G., Fabian A.C., Goyder R., Lasenby A.N., 2003, MNRAS, 344, L22
Miniutti G., Fabian A.C, 2004, MNRAS in press, preprint (astro-ph/0309064)

Nandra K., George I.M., Mushotzky R.F., Turner T.J., Yaqoob T., 1999, ApJ, 523, L17
Parmar A.N. et al. 1997, A&AS, 122, 309
Remillard R., 2001, IAU Circ., 7707, 1
Revnivtsev M., Sunyaev R., 2001, IAU Circ., 7715, 1
Reynolds C.S., Begelman M.C., 1997, ApJ, 488, 109
Reynolds C.S., Wilms J., Begelman M.C., Staubert R., Kendziorra E., 2004, MNRAS in press, preprint (astro-ph/0401305)
Rossi S., Homan J., Miller J.M., Belloni T., 2003, to appear in Proc. of the II *BeppoSAX* Meeting, May 5–8, van den Heuvel E.P.J., in't Zand J.J.M. and Wijers R.A.M.J. eds, Amsterdam, preprint (astro-ph/0309129)
Shih D.C., Iwasawa K., Fabian A.C., 2002, MNRAS, 333, 687
Skibo J.G., 1997, ApJ, 478, 522
Tanaka Y. et al., 1995, Nature, 375, 659
Tanaka Y., Lewin W., 1995, in "X–ray Binaries", Lewin W., van Paradijs J., van den Heuvel E. eds., Cambridge University Press, p. 126
Taylor R.D., Uttley P., McHardy I.M., 2003, MNRAS, 342, L31
Turner T.J. et al., 2002, ApJ, 574, L22
Turner T.J., Kraemer S.B., Reeves J.N., 2004, ApJ in press, preprint (astro-ph/0310885)
van der Klis M., 1995, in "X–ray Binaries", Lewin W., van Paradijs J., van den Heuvel E. eds., Cambridge University Press, p. 252
Wijnands R., Miller J.M., Lewin W.H., 2001, IAU Circ., 7715, 2
Wilms J., Reynolds C.S., Begelman M.C., Reeves J., Molendi S., Staubert R., Kendziorra E., 2001, MNRAS, 328, L27
Yaqoob T., George I.M., Kallman T.R., Padmanabhan U., Weaver K.A., Turner T.J., 2003, ApJ, 596, 85
Young A.J., Ross R.R., Fabian A.C., 1998, MNRAS, 300, L11

Table 1. The 2.5–10 keV spectral analysis with MODEL 1. We do not report in the Table results on the narrow emission lines around 5 keV (NL model in the Table). These are $E_{\rm line} = 5.4 \pm 0.1$ in obs. 1, and $E_{\rm line} = 5.2 \pm 0.2$ in obs. 2 and 3, with an EW of 12 ± 6 eV in obs. 1 and 3 and an upper limit of 15 in obs. 2.

MODEL 1	PHABS × SMEDGE × [PL + DISKBB + NL + LAOR]								
	Γ	$KT_{\rm in}$	$E_{\rm line}$	EW	β	$r_{\rm in}$	$E_{\rm edge}$	$\tau_{\rm max}$	χ^2/dof
2.5–10 keV SPECTRUM (MECS)									
obs. 1	$1.77^{+0.05}_{-0.16}$	0.63 ± 0.03	$6.60^{+0.11}_{-0.10}$	320 ± 60	$4.36^{+0.31}_{-0.19}$	$1.88^{+0.19}_{-0.64}$	$8.3^{+0.2}_{-0.3}$	0.5 ± 0.2	$146.1/147$
obs. 2	$2.69^{+0.38}_{-0.11}$	0.62 ± 0.03	$6.75^{+0.17}_{-0.20}$	340 ± 80	$4.28^{+0.34}_{-0.45}$	$1.70^{+0.62}_{-0.46}$	8.3 ± 0.4	0.5 ± 0.2	$188.4/147$
obs. 3	2.6 ± 0.3	0.60 ± 0.03	$6.87^{+0.1}_{-0.24}$	260 ± 80	5.2 ± 0.3	$2.4^{+2.1}_{-1.0}$	8.2 ± 0.4	0.6 ± 0.2	$138.2/147$

Table 2. The 1.5–200 keV spectral analysis with MODEL 2. The analysis has been restricted to the 1.5–60 keV energy band for obs. 1 (see text for details).

MODEL 2	PHABS × [CUTOFFPL[1] +NL1[2] + RELBLUR[3] (PEXRIV + DISKBB + NL2[2])]								
	Γ	$KT_{\rm in}$	$E_{\rm Fe}$	EW[4]	β	$r_{\rm in}$	R	ξ ($\times 10^4$)	χ^2/dof
1.5–200 keV SPECTRUM (LECS + MECS + PDS)									
obs. 1 (1.5–60 keV)	$1.81^{+0.08}_{-0.09}$	$0.64^{+0.08}_{-0.05}$	$6.48^{+0.12}_{-0.06}$	160 ± 60	3.51 ± 0.15	$1.34^{+0.82}_{-0.10}$	0.80 ± 0.5	0.2 ± 0.2	$402.5/324$
obs. 2	$2.13^{+0.03}_{-0.02}$	0.67 ± 0.02	$6.71^{+0.13}_{-0.09}$	250 ± 80	3.8 ± 0.2	$1.67^{+0.19}_{-0.21}$	2.1 ± 0.5	$1.0^{+0.9}_{-0.2}$	$533.5/434$
obs. 3	2.08 ± 0.05	0.63 ± 0.04	$6.69^{+0.19}_{-0.16}$	190 ± 90	$3.80^{+0.31}_{-0.22}$	$2.10^{+1.20}_{-0.70}$	2.9 ± 1.0	$1.6^{+1.2}_{-0.9}$	$434.8/416$

[1] The parameters of the CUTOFFPL are tied to those of the reflection model PEXRIV
[2] NL1 is the narrow line around 5 keV, while NL2 is affected by relativistic blurring and represents the broad Fe line. In both cases, the width is fixed to zero. Only results on the broad line are reported, those on the narrow lines being identical to the previous 2.5–10 keV analysis (see caption of Table 1).
[3] The relativistic blurring RELBLUR is provided by the kernel of the LAOR model
[4] The Fe line EW (given in eV) is computed with respect to the total underlaying continuum (in Table 3, different ways of computing it are examined)

Table 3. 1.5–200 keV unabsorbed flux of the main spectral components are shown together with the relative reflection and the Fe line EW computed with respect to the PLC only and to the reflection continuum only. Fluxes are in units of 10^{-9} erg/cm^2/s with the exception of the Fe line flux which is in units of 10^{-11} erg/cm^2/s. The line EW is given in eV.

1.5–200 keV FLUXES FROM THE BROADBAND BEST FIT MODELS								
	$F_{\rm tot}$	$F_{\rm DISKBB}$	$F_{\rm PLC}$	$F_{\rm REF}$	$F_{\rm line}$	R	$EW_{\rm PLC}$	$EW_{\rm REF}$
obs. 1	25.0 ± 7.0	1.3 ± 0.6	18.2 ± 3.0	5.4 ± 3.2	$9.4^{+2.4}_{-2.7}$	0.8 ± 0.5	255^{+60}_{-70}	440 ± 120
obs. 2	16 ± 4.0	9.2 ± 0.5	3.2 ± 1.1	3.6 ± 1.2	8.4 ± 2.2	2.1 ± 0.8	820 ± 180	470 ± 120
obs. 3	14.0 ± 2.5	11.8 ± 0.5	1.2 ± 0.8	1.8 ± 1.0	3.1 ± 1.2	2.9 ± 1.0	860 ± 250	370 ± 160